Kinetics of Oligomer-Forming Reactions Involving the Major Functional Groups Present in Atmospheric Secondary Organic Aerosol Particles

Journal:	*Environmental Science: Processes & Impacts*
Manuscript ID	EM-ART-03-2022-000124.R1
Article Type:	Paper

Environmental Significance Statement

Large quantities of volatile organic compounds are emitted from biogenic and anthropogenic sources into the atmosphere. There they are oxidized to lower volatility products that can partition into aerosol particles, where they can undergo accretion reactions to form oligomers. Laboratory measurements of the kinetics of accretion reactions conducted in single organic phases and phase-separated organic/aqueous mixtures containing organic compounds typical of those present in atmospheric aerosol particles provide insight into the accretion reactions that are most likely to occur in the atmosphere, and the effects of water and acid catalysts. The results will help in understanding and modeling processes that influence the composition and properties of aerosol particles, which have important impacts on climate, and human and environmental health.

Kinetics of Oligomer-Forming Reactions Involving the Major Functional Groups Present in Atmospheric Secondary Organic Aerosol Particles

Hannah K. Maben[†,‡] and Paul J. Ziemann[†,‡,*]

Submitted to Environmental Science: Processes & Impacts

† Department of Chemistry, University of Colorado, Boulder, Colorado 80309, United States

‡ Cooperative Institute for Research in Environmental Sciences (CIRES), Boulder, Colorado 80309, United States

* Corresponding Author: Paul J. Ziemann

*Phone: 303-492-9654; fax: e-mail: paul.ziemann@colorado.edu

Abstract: Atmospheric organic aerosol particles impact climate as well as human and environmental health. Secondary organic aerosol (SOA), which is formed by the gas-to-particle partitioning of products of the oxidation of volatile organic compounds (VOCs) emitted from biogenic or anthropogenic sources, contributes a large fraction of this material. In the particle phase, these products can undergo accretion reactions to form oligomers that impact the formation, composition, and chemical-physical properties of aerosols. While these reactions are known to occur in the atmosphere, data and models describing their kinetics and equilibria are sparse. Here, reactions of compounds containing potentially reactive hydroperoxide, hydroxyl, carboxyl, aldehyde, and ketone groups were investigated in single and phase-separated organic/aqueous mixtures in the absence and presence of a sulfuric acid catalyst. Compounds containing these groups and a nonreactive UV-absorbing nitrate group were synthesized and their reactions and products were monitored and characterized using high-performance liquid chromatography with UV detection (HPLC-UV), electrospray ionization-mass spectrometry (ESI-MS), and attenuated total reflectance-Fourier transform infrared (ATR-FTIR) spectroscopy. Reactions were observed between hydroperoxides and aldehydes to form peroxyhemiacetals, and between carboxylic acids and alcohols to form esters, and their rate and equilibrium constants were determined. No reactions were observed in other mixtures, indicating that under the conditions of these experiments only a few reaction pathways form oligomers. Reactions were also conducted with probe compounds and SOA formed in an environmental chamber reaction of α-pinene with O_3 SOA. Whereas in a previous study we observed a rapid hydroperoxide reaction in this SOA, among the other compounds studied here only alcohols reacted. These results provide insight into the types of accretion reactions that are likely to occur in atmospheric aerosols, and the rate and equilibrium constants can be used to better model SOA chemistry.

1 Introduction

Atmospheric aerosol particles are readily inhalable, they efficiently scatter and absorb light and act as nuclei for cloud formation, and they provide surfaces and condensed phases for chemical reactions.[1,2] As a result, they negatively impact human and environmental health, decrease visibility, and affect atmospheric composition and the global climate.[1–3] A large fraction of atmospheric aerosol mass is organic matter derived from the oxidation of volatile organic compounds (VOCs)[4,5] that are emitted into the atmosphere from biogenic and anthropogenic sources, with biogenic emissions contributing ~90% of non-methane VOCs globally and anthropogenic emissions being more important in urban areas.[6,7] In general, VOC oxidation leads to the addition of functional groups, primarily carbonyl, hydroxyl, carboxyl, hydroperoxide, ester, and nitrate, and often fragmentation of the carbon chain.[6] The addition of these functional groups results in products that are more polar, less volatile, and more water soluble, and thus have a greater tendency to partition to particles to form secondary organic aerosol (SOA).[8,9] Once in the particles, carbonyl, hydroxyl, carboxyl, and hydroperoxide groups can participate in accretion reactions in which covalent bonds are formed that link monomers into larger, less volatile oligomers.[8,9] These oligomers impact the formation and composition of SOA, as well as the chemical-physical properties of aerosol, which in turn affects their behavior in the atmosphere.[10]

Laboratory studies and field studies employing various types of mass spectrometry have observed that oligomers are present in SOA formed from the oxidation of most VOCs, and can contribute a large fraction of the organic mass.[10] Unfortunately, identification of oligomer structures is usually not possible, due to the complexity of the SOA composition and reaction mechanisms and the fact that in most cases the chemical information available is limited to molecular formulas. Some studies, however, especially those that combined chromatographic or thermal separation methods with mass spectrometry and/or involved interpretation of mass spectra with relatively simple patterns, have provided (in our opinion) convincing structural assignments that demonstrate that a variety of accretion reactions can occur in SOA to form a few classes of oligomers. Examples include peroxyhemiacetals[11,12] and esters[13] from reactions of alkenes with O_3; esters and hemiacetals from reactions of isoprene with OH radicals;[14,15] acetals[16] and aldols[17] from the reactions of aromatic hydrocarbons with OH radicals; and acetals from reactions of monoterpenes with NO_3 radicals.[18,19]

Although it is now widely acknowledged that accretion reactions are important in SOA formation, they are rarely included in models. Whereas considerable progress has been made to develop explicit VOC oxidation mechanisms, such as the Generator of Explicit Chemistry and Kinetics of Organics in the Atmosphere (GECKO-A)[20] and the Master Chemical Mechanism (MCM),[21] and these mechanisms and others[22,23] have been combined with gas-particle partitioning theory to predict the formation of SOA in the laboratory[24,25] and the ambient atmosphere,[26,27] the models usually ignore or include limited representations of accretion reactions.[22,23] This is in large part because of the lack of data on the kinetics and equilibria of these reactions, which are often acid catalyzed and could occur in organic or aqueous particles, or in particles containing phase-separated organic/aqueous mixtures of chemical components.[28,29] Studies of accretion reactions published in the organic chemistry literature can be highly informative regarding products and mechanisms, but the investigated compounds and conditions under which rate and equilibrium constants were measured often do not allow easy application to the atmosphere (see the review by Ziemann and Atkinson[9] for a brief discussion of this literature and its potential relevance to SOA chemistry).

In the present study we build on the methods and results of a recent study in which we measured the rate and equilibrium constants for the formation of peroxyhemiacetals from the reaction of a hydroperoxide with a single aldehyde and with aldehydes present in SOA formed from the reaction of α-pinene with O_3.[30] The approach involves the use of nitrate-labelled probe compounds that absorb in the UV, thus allowing their reaction and the formation of products to be monitored using HPLC-UV. The accretion reactions investigated are shown in Figure 1. One set of experiments was conducted in a single organic phase in dry air without sulfuric acid (except in one experiment), representing the end of the spectrum of conditions where no potential acid catalyst was present and accretion reactions did not compete with hydrolysis. Such neutral conditions apply to the upper end of the pH range for the occurrence of these reactions, for example in clouds, sea spray, or aerosol particles exposed to high concentrations of ammonia, which neutralizes acidity.[31] A second set of experiments was conducted in phase-separated organic/aqueous mixtures without and with 3.0 M sulfuric acid (pH ~–0.7), which because of its hygroscopicity will take up water in the atmosphere to form aqueous solutions.[2] Aerosol particles with acidity comparable to this were observed in the Southern Oxidants and Aerosol Study conducted in the southeast US in 2013, where sulfate was a significant component and pH ranged from ~0.5–3, with an average pH~1.[32] And a recent analysis of measurements made in eleven aircraft campaigns showed a decrease of aerosol pH from ~3 in polluted areas to ~–1 in remote areas, with a corresponding decrease in the ammonia balance from ~1 to ~0.[33] The presence of organic components in these particles often leads to phase-separated organic/aqueous mixtures,[28,29] and we have recently shown that sulfuric acid can partition to the organic phase in such mixtures,[34] where it can possibly catalyze accretion reactions.

2 Materials and methods

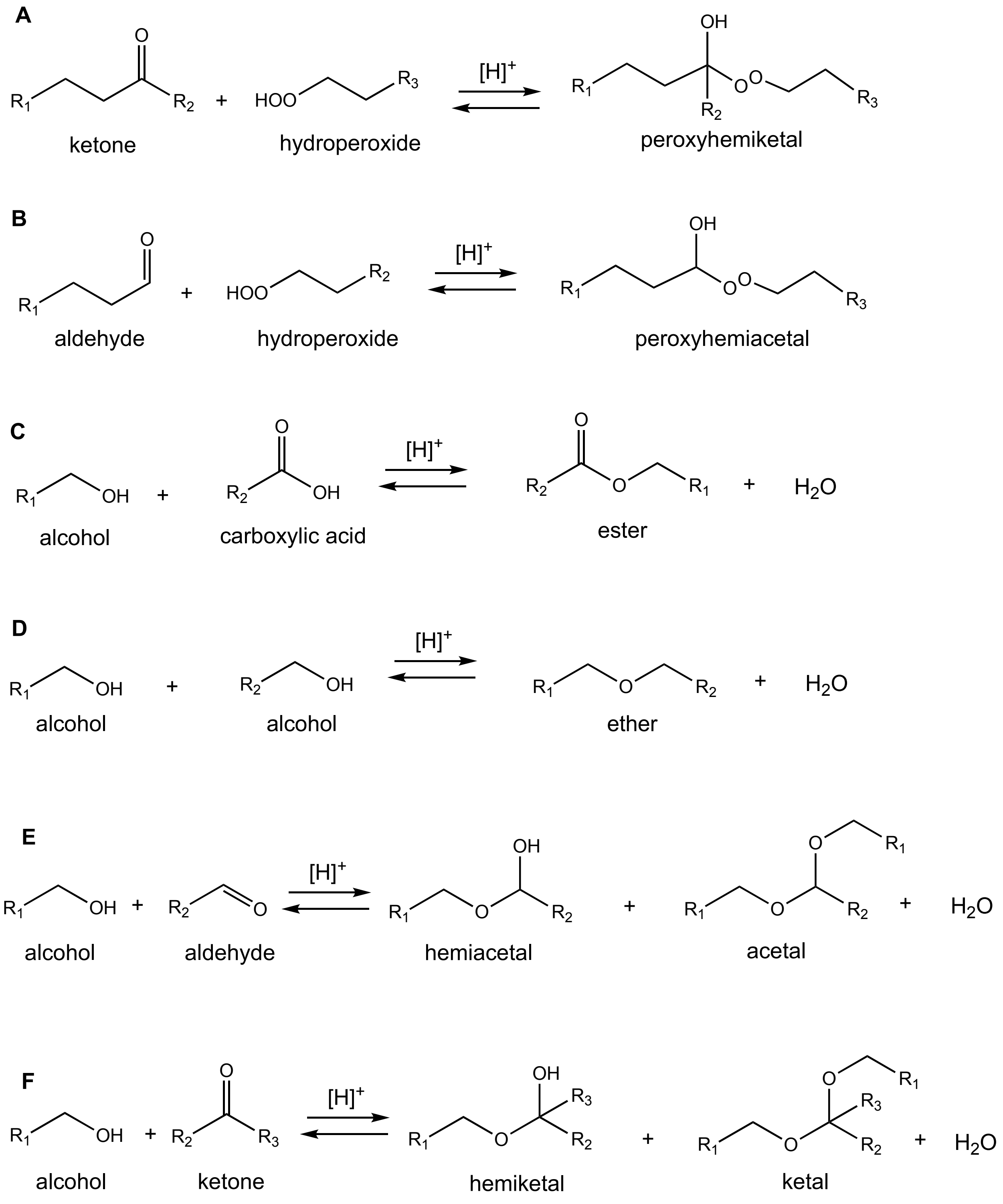

Figure 1. Accretion reactions investigated in this study.

2.1 Materials

The following chemicals with stated purities and suppliers were used in this study: *trans*-7-tetradecene (97%), nonanal (95%), 3-decanone (98%), 11-hydroxyundecanoic acid (96%), 1-octanol (99+%), 1,10-decanediol (98%), 1,2-octanediol (purity N/A), and 1,2-decanediol (98%) from Aldrich; 1,4-butanediol (99+%), α-pinene (99+%) and acetonitrile (HPLC grade) from Sigma-Aldrich; 6-hydroxy-5-decanone (purity N/A) and 5-hydroxy-2-pentanone (purity N/A) from TCI; sulfuric acid (95.3 w/w%) and water (HPLC grade) from Fisher; ultrahigh purity (UHP) O_2 and N_2 from Airgas; and ethyl acetate (99.5%) from EMD Millipore. Ozone was produced from UHP O_2 using a DelOzone LG7 ozone generator and N_2O_5 was synthesized according to the method described in Atkinson et al.[35]

2.2 Synthesis of multifunctional organic nitrate probe compounds

The probe compounds synthesized for this study included a 5,10-hydroperoxynitrate (HPN); 1,11-carboxylic acid nitrate (CAN); 1,10-hydroxynitrate (HN); 5,6-carbonylnitrate (βCN); and a mixture of 1,2- and 2,1-hydroxynitrate isomers (βHN). The HPN was synthesized using the two-step synthesis shown in Figure 2A.[30] First, N_2O_5 was bubbled through a solution of 1,4-butanediol in acetonitrile to produce a mixture of unreacted 1,4-butanediol, 1-hydroxy-4-nitrooxybutane, and 1,4-dinitrooxybutane. Next, 7-tetradecene (a symmetric alkene was used to increase product yield) was dissolved in acetonitrile with sonication, the solution was combined with the mixture from the first step, and 10% O_3/O_2 was bubbled through the solution at ~1 L min^{-1} for 5 min to form the HPN by reaction of the 1-hydroxy-4-nitrooxybutane with the C_7 Criegee intermediate.[30] The CAN, HN, βCN, and βHN probe compounds were synthesized as shown in Figures 2B–E by bubbling N_2O_5 through acetonitrile solutions containing 11-hydroxyundecanoic acid; 1,10-decanediol; 6-hydroxy-5-decanone; and 1,2-decanediol, respectively. The resulting mixtures all contained the nitrate probe compound of interest (two

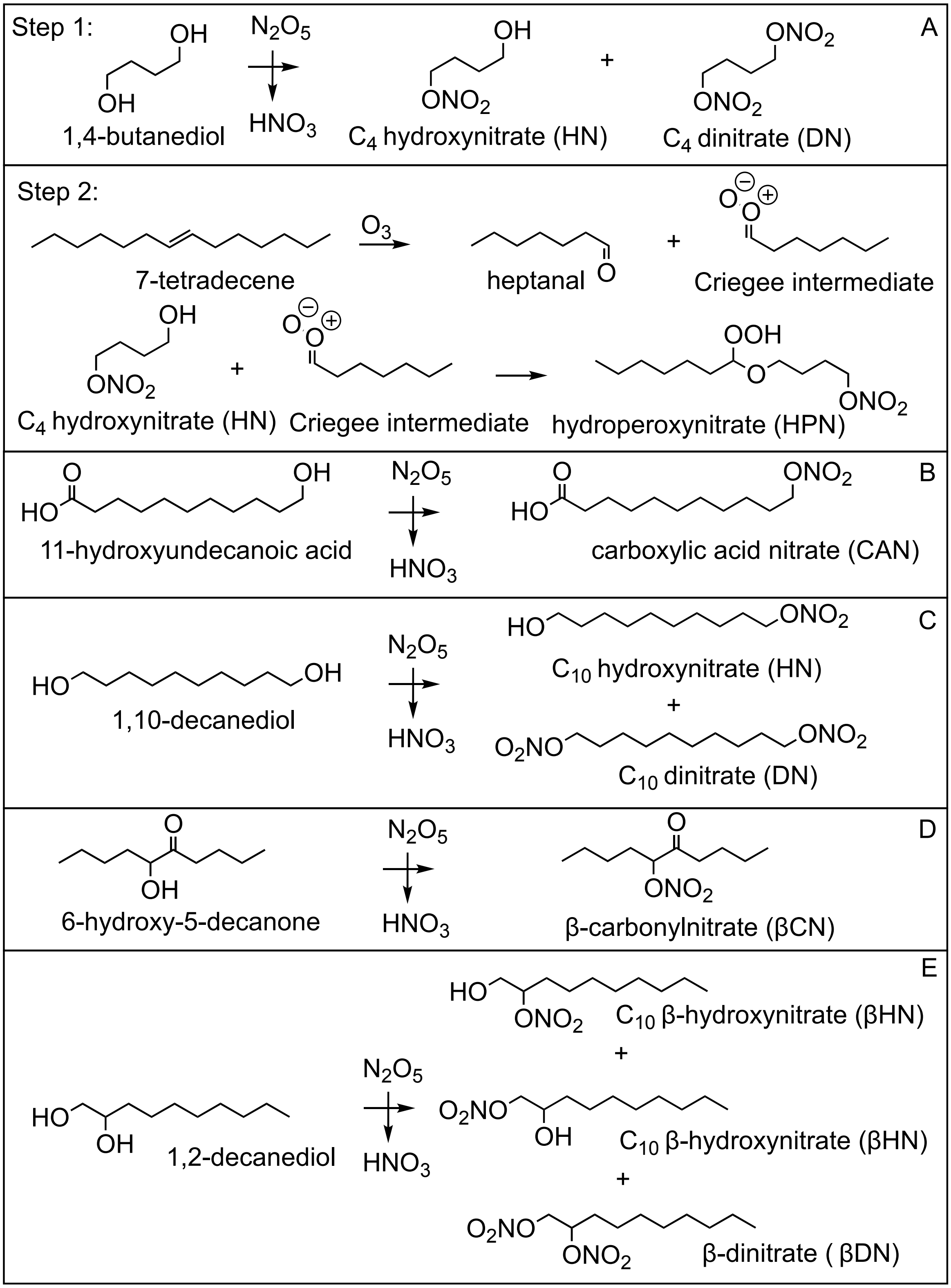

Figure 2. Mechanisms of synthesis of the (A) HPN, (B) CAN, (C) HN, (D) βCN, and (E) βHN multifunctional organic nitrate probe compounds.

isomers for the βHN), unreacted compound, and nitric acid. In the HN and βHN a dinitrate was also formed. These solutions were purified by reversed-phase high performance liquid chromatography (HPLC) using a Shimadzu Prominence HPLC with a Zorbax Eclipse XDB-C_{18} semi-preparative column (9.4 x 250 mm, 5 μm particle size) for high throughput, and a Nexera X2 SPD-M30A UV/vis photodiode array detector. Absorbance was measured at 210 nm, where nitrate groups absorb strongly.[36] Example chromatograms are shown in Figure 3. The HPN, CAN, HN, βCN, and βHN fractions were collected and used as probe compounds to monitor the reaction in the kinetics experiments.

2.3 Acid partitioning measurements

The partitioning of sulfuric acid between 1-octanol and water in a phase-separated organic/aqueous mixture was measured using the shake-flask method.[37,38] 1-Octanol served as a surrogate for the reactant organic compounds that were present in large excess relative to the probe compound in the kinetics experiments, and the aqueous phase consisted of a series of sulfuric acid/water solutions with acid concentrations ranging from 0 to 3.0 M. Aliquots of the organic and aqueous phases were added to test tubes and then mixed by vortexing, followed by centrifugation. The organic phase was sampled with a syringe, transferred to a pre-weighed vial, and then ammonia gas was bubbled through the solution to convert the sulfuric acid to insoluble ammonium sulfate salt. Since the organic phase was not sufficiently volatile to be removed by evaporation, the vials were placed in a stream of N_2 to evaporate water until a constant mass was achieved. A blank experiment was also conducted using 1-octanol and water without sulfuric acid, and the mass of this sample was used to correct for the mass of 1-octanol in the ammonium sulfate/octanol samples. The mass of ammonium sulfate and added sulfuric acid were used to calculate the ratio of the concentration of sulfuric acid in the organic and aqueous phases, which

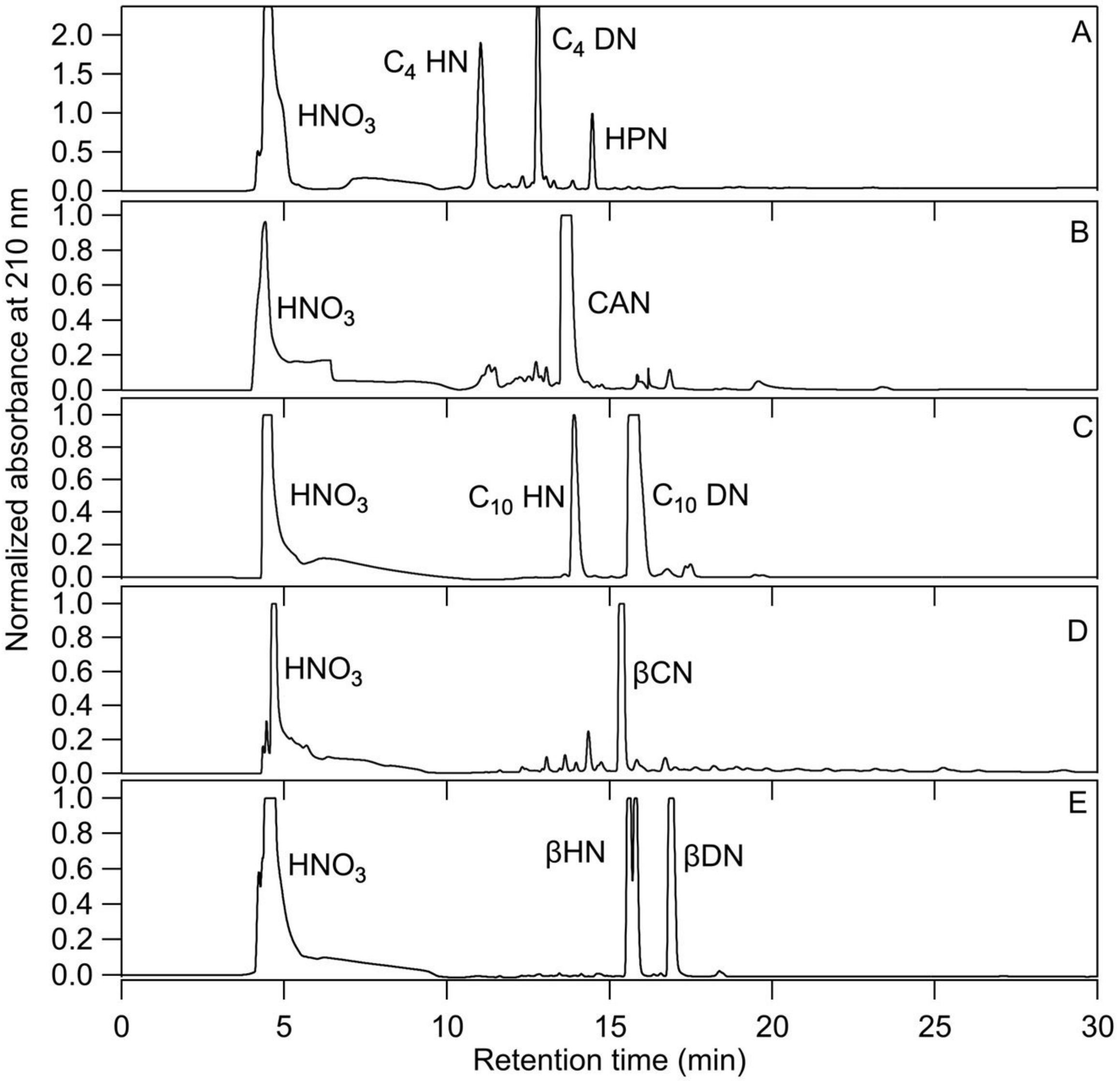

Figure 3. HPLC chromatograms of the fractionated synthesis mixtures of the (A) HPN, (B) CAN, (C) HN, (D) βCN, and (E) βHN multifunctional organic nitrate probe compounds used to collect purified fractions for kinetics experiments.

was then used to determine the distribution coefficients as described below. Samples were weighed on a Mettler Toledo XS3DU Microbalance that is accurate to ±0.5 µg. The acidity of the organic phase was also measured over a larger concentration range using an EL20-BASIC Mettler Toledo pH meter. Aqueous solutions containing 0 to 3.0 M concentrations of sulfuric acid were prepared and then 4.0 mL of each solution and 0.25 mL of 1-octanol were added to a test tube and mixed by vortexing for 30 s. The organic layer was removed using a syringe and the pH of this phase was measured by submerging the probe of the pH meter.

2.4 Kinetics experiments

Four types of experiments were conducted to measure reaction rate and equilibrium constants (though not for all reactions): a single organic phase, a single organic phase containing sulfuric acid, and an organic/aqueous phase-separated mixture without and with sulfuric acid. Six solution reaction vials were prepared for each experiment, with the non-probe reactant being added in large excess (25× or 100×) in order to achieve pseudo-first-order kinetics conditions. The moles of reactants added as either pure components or acetonitrile solution were as follows: 1.9×10^{-8} of HPN and 5.2×10^{-7} of aldehyde (nonanal) or ketone (3-decanone), similar to previous experiments;[30] 5.0×10^{-7} of CN and 5.0×10^{-5} of alcohol (1-octanol); 1.9×10^{-8} of HN and 5.2×10^{-7} of alcohol (1-octanol), aldehyde (nonanal), β-hydroxyketone (6-hydroxy-5-decanone), or δ-hydroxyketone (5-hydroxy-2-pentanone, which also exists as a cyclic hemiacetal), or an additional 1.9×10^{-8} of HN; 1.9×10^{-8} of βNC and 5.2×10^{-7} of alcohol (1-octanol) or β-diol (1,2-octanediol); and 1.9×10^{-8} of βHN and 5.2×10^{-7} βNC. After mixing the reactant solutions the volume ranged from ~20–200 μL, and after drying from ~0.05–5 μL.

2.4.1 Reactions in a single organic phase

The two reactants were added to each glass vial using a glass syringe, followed by 20 s of mixing with a vortexer and evaporation of the acetonitrile in a stream of N_2 so that only the reactants remained. Solutions of a single reactant in acetonitrile were also added separately to vials, dried with N_2, and then weighed to verify that no reactants were lost during drying. The six reaction solution vials were capped and allowed to react for 0 min, 15 min, 30 min, 1 h, 4 h, and 24 h, which is a relevant timescale for atmospheric particle-phase reactions.[39] After the specified time period, 100 μL of acetonitrile was added, the solution was injected onto the HPLC, and the nitrate group absorption at 210 nm was monitored. The mobile phase was acetonitrile/water, starting at 40% acetonitrile and increasing linearly to 100 % acetonitrile over 40 or 45 min. An acid catalyzed experiment was also conducted for the CAN reactions, where 25 μL of a 0.005 M sulfuric acid solution in acetonitrile was added without drying.

2.4.2 Reactions in phase-separated organic/aqueous mixtures without and with sulfuric acid catalyst

The reactants were combined as described above, and after drying, HPLC water or an aqueous solution containing 3.0 M sulfuric acid with the same volume as the probe compound solution was added to create a phase-separated aqueous/organic mixture.

2.4.3 Reactions in a phase-separated SOA/aqueous mixture without and with sulfuric acid catalyst

These experiments were similar to those described above, but the organic phase was SOA produced from the reaction of α-pinene with O_3. Previous functional group analysis by our group showed that this SOA contains significant amounts of hydroxyl and carbonyl groups that can potentially react with probe compounds.[40] The SOA was produced in a 7.3 m^3 FEP Teflon environmental chamber that was operated at room temperature and pressure (~25 °C, ~630 Torr) and filled with clean, dry air supplied by two AADCO clean air generators (<5 ppbv hydrocarbons, <1% RH). Approximately 10 ppm of α-pinene was added to the chamber from a heated glass bulb in a flow of N_2 and then ~10 ppm of O_3 to initiate the reaction. A scanning mobility particle sizer (SMPS) was used to monitor the SOA mass concentration, which reached a maximum in ~1 h. The SOA was then collected on pre-weighed 0.45 μm PTFE filters for 2 h by sampling chamber air at 14 L min^{-1}. The filters were extracted three times with 5 mL ethyl acetate to obtain ~20 mg of SOA for use in the kinetics experiments.

2.4.4 Reaction product analysis

Products of synthesis reactions and kinetics experiments were analyzed after HPLC fractionation and collection using an Agilent 6220A ESI-ToF-MS and Agilent Cary 360 ATR-FTIR spectrometer. In the ESI-MS analysis compounds were detected as their Na^+ adducts and molecular formulas were assigned within 5 ppm.

2.4.5 Safety precautions

All syntheses of probe compounds employing N_2O_5 and any procedure that involves solvent evaporation should be conducted in a fume hood, and for all syntheses and experiments appropriate personal protective equipment should be worn.

3 Results and discussion

3.1 HPN reactions

As shown in Figure 4A, where the ratio of $[HPN]_t/[HPN]_o$ measured over 24 h is plotted against time, no reaction was observed for the phase-separated organic/aqueous mixture of HPN and 3-decanone when the aqueous phase was pure water or a 3.0 M solution of sulfuric acid. The pH of this solution calculated using E-AIM (http://www.aim.env.uea.ac.uk/aim/aim.php)[41,42] is –0.7, at the low end of values measured in aerosol particles in remote regions of the atmosphere.[33] Based on our previous measurements of the partitioning of sulfuric acid between 2-hexanone and water,[34] we would expect ~1% of the sulfuric acid to partition to the organic phase in dissociated form as $H^+ + HSO_4^-$. These results thus indicate that hydroperoxides do not react with ketones, even in the presence of a strong acid catalyst, similar to our previous measurements for the reaction of the HPN and 3-decanone in the presence of an organic acid catalyst.[30] The constant

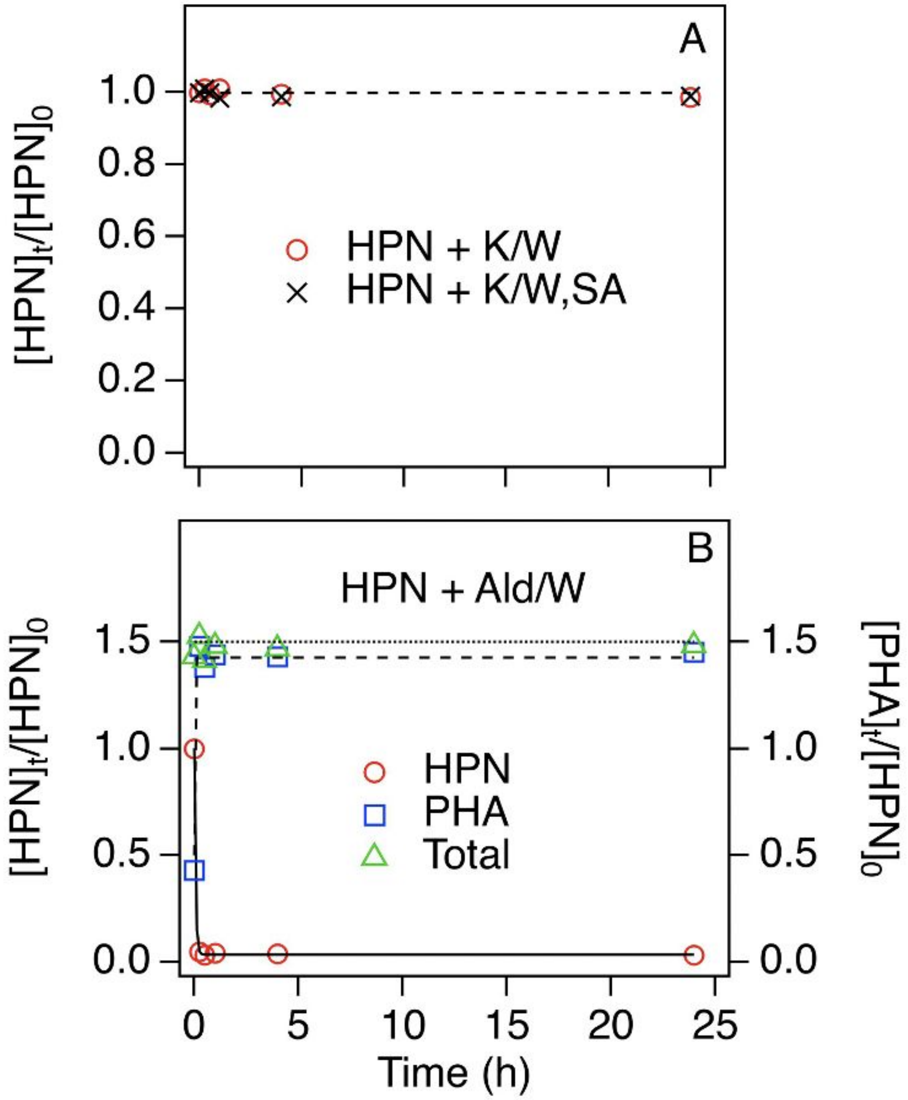

Figure 4. (A) Time profiles of the ratio $[HPN]_t/[HPN]_0$ for reactions of HPN with 3-decanone (K) in phase-separated organic/aqueous mixtures with the aqueous phase being water (W) or a 3.0 M solution of sulfuric acid in water (W, SA). The dashed lines are drawn at $[HPN]_t/[HPN]_0 = 1$. (B) Time profiles of the ratio $[HPN]_t/[HPN]_0$, the ratio of the PHA product $[PHA]_t/[HPN]_0$, and the sum of the ratios, for reaction of HPN with nonanal (Ald) in a phase-separated organic/aqueous mixture with the aqueous phase being water (W). Results in panels A and B are for single experiments.

HPN signal also indicates that the HPN is stable when exposed to water or a 3.0 M aqueous solution of sulfuric acid.

Conversely, as shown in Figure 4B, when the HPN was mixed with nonanal in the phase-separated organic/aqueous mixture with an aqueous phase of pure water, the HPN peak in the HPLC chromatogram rapidly decreased due to reaction with nonanal to form a peroxyhemiacetal (PHA). This product was identified in our previous study using ESI-MS.[30] The reaction went almost to completion, and equilibrium was reached in ~5 min. The sum of the HPN and PHA product signals were constant over time, indicating no loss of the nitrate group from the HPN or PHA, but was greater than 1. We attribute this excess signal to an increasing baseline in the HPLC chromatogram, which added to the PHA signal. The time profile of $[\mathrm{HPN}]_t/[\mathrm{HPN}]_o$ was fit to the equation

$$\frac{[A]_t}{[A]_o} = \frac{[A]_{eq}}{[A]_o} + \left(1 - \frac{[A]_{eq}}{[A]_o}\right) exp^{-k't} \tag{1}$$

which is appropriate for a pseudo-first-order reaction that reaches an equilibrium between reactants and product. In this equation, $[A]_t$ is the concentration of the probe compound at time t, $[A]_{eq}$ is the concentration at equilibrium, and $[A]_o$ is the initial concentration. Concentrations were normalized to the initial concentration, and k' is the pseudo-first order rate constant given by the equation

$$k' = k_{f,u}[C = O] + k_{r,u} \tag{2}$$

where $k_{f,u}$ and $k_{r,u}$ are the forward and reverse rate constants for the uncatalyzed reaction and [C=O] is the concentration of nonanal. The equilibrium constant, K_{eq}, can be obtained from measured quantities using the equation

$$K_{eq} = \frac{k_{f,u}}{k_{r,u}} = \frac{\left(\frac{[HPN]_o}{[HPN]_{eq}} - 1\right)}{[C = O]} \tag{3}$$

Unfortunately, because of the difficulty in measuring the HPN concentration for time periods less than 5 min, and the rapid rate of this reaction, the fit of Equation 1 to the data during the first 5 min of reaction is highly uncertain (Figure S1). As a result, uncertainties on values of $[HPN]_{eq}/[HPN]_o$ and k' obtained from the fit are so large that the values are not reliable. Instead, the flat region of the curve between 0.5 and 24 h in Figure 4B was used to calculate an average value and standard deviation of $[HPN]_{eq}/[HPN]_o = 0.034 \pm 0.002$. When used with [C=O] = 5.8 M in Equation 3, this gives a value of $K_{eq} = 4.9 \pm 0.3$ M^{-1}, which is similar to the value of K_{eq} = 6.0 M^{-1} obtained in our previous measurements of the kinetics of this reaction in the absence of water.[30] That reaction was only slightly slower than the reaction in the absence of water, but enough so that the kinetics could be followed more easily. Based on those results we can place lower limits on the values of $k_{f,u,}$ and $k_{r,u}$ for the reaction in the presence of water of 1.5 M^{-1} h^{-1} and 0.24 h^{-1}.[30] The water (which has a solubility of 0.4 M in a C_9 cyclic aldehyde[43]) appears to slightly accelerate the reaction, even though water competes with the HPN by reacting with nonanal to form a gem-diol ($CH_3(CH_2)_7CH(OH)_2$).[44]

3.2 CAN reactions

Experiments were conducted with the CAN probe compound and 1-octanol in a single organic phase without sulfuric acid, in an acetonitrile solution with sulfuric acid, and in a phase-separated organic/aqueous mixture with sulfuric acid. The concentration of sulfuric acid in the acetonitrile solution was determined from the amount added and volume of acetonitrile, whereas the concentration in the organic phase (1-octanol) in the phase-separated mixture was determined by an acid partitioning experiment with 3.0 M sulfuric acid and 1-octanol and pH measurements as described above. The measured ratio of the total concentration of undissociated and dissociated acid in the organic phase (T_{org}) to the total concentration of acid in the aqueous phase

(T_{aq}), R, was plotted against T_{aq} in Figure 5A to determine the concentration of sulfuric acid in the organic phase and the extent of dissociation according to the equation

$$R = \frac{T_{org}}{T_{aq}} = \frac{D_{un}}{K_{a,aq}} T_{aq} + D_{diss} \tag{4}$$

where the slope of the line corresponds to $\frac{D_{un}}{K_{a,aq}}$ and the y-intercept is equal to D_{diss}.[34] In this equation D_{un} and D_{diss} are the distribution coefficients for partitioning of undissociated and dissociated acid between the organic and aqueous phases and $K_{a,aq}$ is the acid dissociation constant in the aqueous phase. Because the data are quite scattered and a negative slope is physically unrealistic, all the values of R were averaged to obtain a line with zero slope and y-intercept = D_{diss} = 0.09. Since no SO_4^{2-} is expected to partition to the organic phase because of the difficulty of solvating the divalent ion, this value of D_{diss} describes the partitioning of HSO_4^- and so was corrected by multiplying by a factor of 1.5 to obtain D_{diss} = 0.14.[34] Combining this value with the total concentration of sulfuric acid in both phases gives $[HSO_4^-]_{org} = [H^+]_{org}$ = 0.37 M. This concentration can be compared to the value obtained by submerging a pH probe in the organic phase for a range of sulfuric acid concentrations and assuming $pH_{org} = [H^+]_{org}$. Although measurements of pH in organic solvents can be difficult to interpret,[45] the presence of 2.2 M water in the 1-octanol (the solubility of water in 1-octanol[46]) improves the validity of this measurement. As shown in Figure 5B, $[H^+]_{org}$ increases linearly with the total concentration of sulfuric acid (equal to the initial concentration in the aqueous phase since the since the organic and aqueous phase volumes were equal), and the fitted line gives a value of $[H^+]_{org}$ = 0.25 M for a total acid concentration of 3.0 M. The two values of $[H^+]_{org}$ agree within ~50%, adding confidence to the measurements, and because the pH measurements appear to be higher quality we assume that $[H^+]_{org}$ = 0.25 M in the phase-separated mixture.

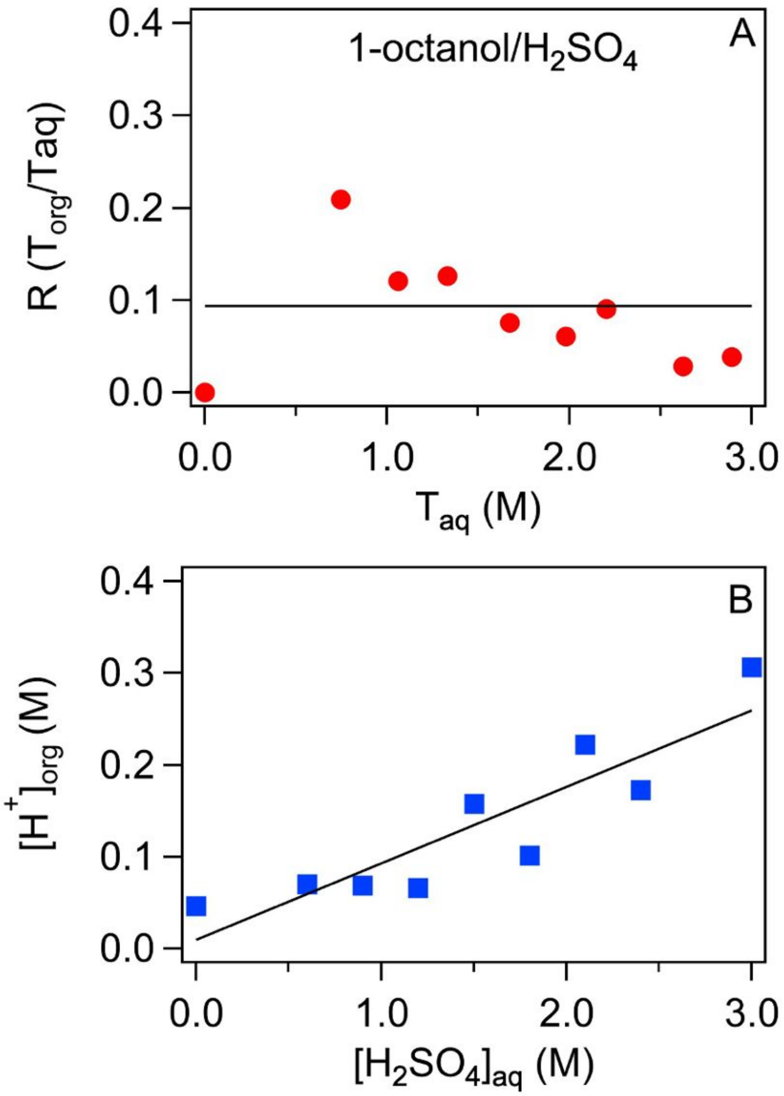

Figure 5. (A) Ratios of organic phase acid/aqueous phase acid, R(T_{org}/T_{aq}), measured for H_2SO_4 as a function of the aqueous phase acid concentration with 1-octanol as the organic phase. The line represents the averaged R values taken to be the y-intercept. (B) Measured organic phase H^+ concentrations. The line is the linear least squares fit to the data.

Results of experiments conducted with the CAN probe compound and 1-octanol to investigate the reaction of a carboxylic acid with an alcohol to form an ester are shown in Figure 6. In the experiment with only CAN and 1-octanol the CAN peak in the HPLC chromatogram remained constant over 24 h (Figure 6A) and no product peaks appeared, indicating that no ester formed and that the CAN was stable. Conversely, when the CAN was mixed with 1-octanol in

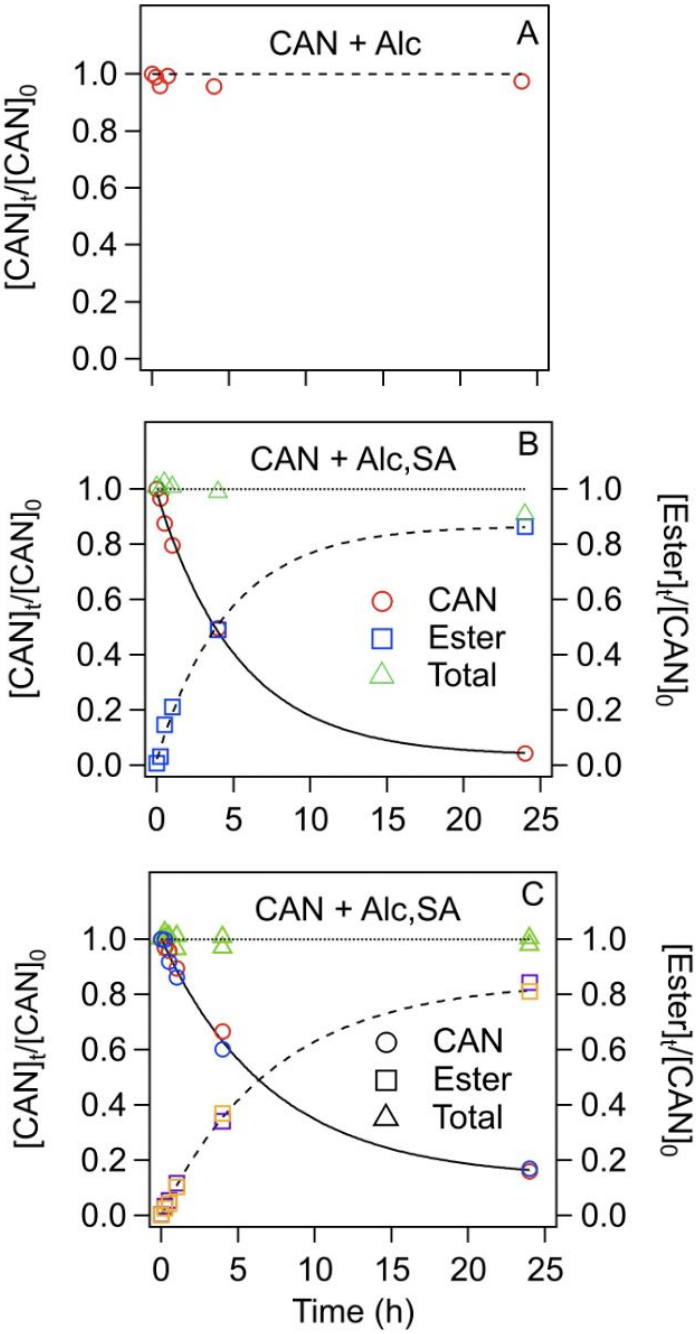

Figure 6. Time profiles of the ratios $[CAN]_t/[CAN]_0$ and $[Ester]_t/[CAN]_0$ and the total $[CAN]_t/[CAN]_0 + [Ester]_t/[CAN]_0$ for reactions of CAN with 1-octanol (Alc) to form an ester in (A) a single organic phase, (B) a single organic phase containing 0.005 M sulfuric acid (SA), and (C) a two-phase organic/aqueous mixture with the aqueous phase being a 3.0 M solution of sulfuric acid in water (W, SA). The dashed line corresponds to $[CAN]_t/[CAN]_0 = 1$ in panel A and the curves in panels B and C are least-squares fits of $[CAN]_t/[CAN]_0$ and $[Ester]_t/[CAN]_0$ to the exponential equation given in the text. Results in panels A and B are for single experiments, and the two values for each time point in panel C are from two separate experiments.

the presence of 0.005 M sulfuric acid in a single-phase solution of acetonitrile (in order to compare with the results described below for the phase-separated organic/aqueous mixture with sulfuric acid, and with the literature), the peak decreased over 24 h to an equilibrium value close zero, indicating a near-complete reaction in this time period (Figure 6B). The time profile of $[CAN]_t/[CAN]_o$ was fit to Equation 1 to obtain a value of k' = 0.19 h^{-1}, where it was assumed that $[CAN]_{eq} = 0$ since the reaction was conducted in the absence of water and therefore no reverse reaction could occur to establish a non-zero equilibrium CAN concentration. For this reaction, which is assumed to be catalyzed by H^+ and in which the rates of the reverse reaction and the uncatalyzed reaction are both zero, k' is given by the equation

$$k' = k_{f,c}[H^+][OH] \tag{5}$$

where [OH] = 6.4 M is the concentration of hydroxyl groups (equal to the 1-octanol concentration), $[H^+] = 0.005$ M is the concentration of H^+ assuming that all the added H_2SO_4 dissociated to H^+ and HSO_4^-, and $k_{f,c}$ is the forward catalytic rate constant. The assumption regarding dissociation of the H_2SO_4 is based on the observation that a measurement of the pH with pH paper (used because in this organic phase the pH meter would not provide a reading) indicated pH = 0–3. The value of $k_{f,c}$ obtained was 5.9 $M^{-2\;-1}$, which is similar to the value of 3.1 M^{-2} h^{-1} measured by Fairclough and Hinshelwood[47] for the reaction of palmitic acid in methanol in the presence of 0.005 M HCl, which is known to be fully dissociated in that alcohol. This agreement suggests that our assumption regarding the dissociation of HSO_4^- is reasonable, although it must be noted that acetonitrile and methanol will have different solvation properties for the reactants and products that will also affect the reaction kinetics.[48]

When the CAN was mixed with 1-octanol in a phase-separated organic/aqueous mixture where the aqueous phase was a 3.0 M solution of sulfuric acid, the CAN peak again decreased over 24 h, but less than in the single-phase reaction (Figure 6C). The $[CAN]_t/[CAN]_o$ time profile was fit to Equation 1 to obtain values of k' = 0.14 ± 0.01 h^{-1} and $[CAN]_{eq}/[CAN]_o$ = 0.11 ± 0.01. The uncertainties were obtained from the fit to the data from two separate experiments, and were used to estimate uncertainties for the rate and equilibrium constants. For this catalyzed reaction, where the rate of the uncatalyzed reaction was again zero but the reverse reaction was no longer zero because of the presence of water, k' is given by the equation

$$k' = k_{f,c}[H^+][OH] + k_{r,c}[H^+][H_2O] \qquad (6)$$

where $k_{f,c}$ and $k_{r,c}$ are the forward and reverse catalytic rate constants for the reaction and [OH] = 6.4 M is the concentration of 1-octanol and $[H^+]$ = 0.25 M. Equation 3 becomes

$$K_{eq} = \frac{k_{f,c}}{k_{r,c}} = \frac{\left(\frac{[CAN]_o}{[CAN]_{eq}} - 1\right) * [H_2O]}{[OH]} \qquad (7)$$

where $[H_2O]$ = 2.2 M is the concentration of water. The calculated values of K_{eq}, $k_{f,c}$ and $k_{r,c}$ were then 2.8 ± 0.3, 0.08 ± 0.03 M^{-2} h^{-1}, and 0.03 ± 0.01 M^{-2} h^{-1}. The value of 2.9 for the equilibrium constant is similar to the value of 1.5 measured by Hassan and Vinjamur[49] for the reaction of oleic acid with methanol in the presence of sulfuric acid at 40 °C, and to the values of 4–11 reported by Lee et al.[50] for the formation of esters from a series of aliphatic carboxylic acids and alcohols. The forward catalytic rate constant of 0.08 M^{-2} h^{-1} is much smaller than the 5.9 and 3.1 M^{-2} h^{-1} values measured for the reactions in acetonitrile and methanol. This can be attributed to the presence of water in the solution, which preferentially solvates H^+ and reduces its catalytic activity.[51,52] In a study of ester formation from the reaction of acetic acid and methanol in the presence of sulfuric acid, Liu et al.[52] observed that adding water to the solution decreased the catalytic rate constant significantly. For example, for 2.9 M water (comparable to the 2.2 M in our solution) they measured a catalytic rate constant of 1.0 M^{-2} h^{-1}, almost an order of magnitude less than the value of 8.1 M^{-2} h^{-1} measured by Smith[51] using an HCl catalyst without water.

For both the acid catalyzed reactions a product peak appeared in the HPLC chromatogram at a retention time of ~34 min and increased in intensity as the CAN reacted, as shown in Figure 7A for the phase-separated organic/aqueous mixture. Based on the ATR-FTIR spectrum (Figure 7B) and ESI mass spectrum (Figure 7C), the product was assigned to the C_{19} ester that was expected to be formed from the reaction of the CAN and 1-octanol. The presence of the C=O and the three distinct O–NO_2 stretches and absence of an O–H stretch from the CAN or 1-octanol is consistent with the ester, and the mass spectrum shows Na^+ adducts at *m/z* 382.2553 and 741.5204, which are within 5 ppm mass accuracy of the values expected for the ester monomer and a dimer, with the latter being formed in the ESI source. There were no other peaks in the chromatogram, indicating that this was the sole product of the reaction.

3.3 HN, βHN, and βCN reactions

In addition to reacting with carboxylic acids to form esters, alcohols can react with alcohols, aldehydes, and ketones to form ethers, hemiacetals and acetals, and hemiketals and ketals, respectively, by the reactions shown in Figure 1. The rates of these reactions can be enhanced by the presence of another functional group, such as a hydroxyl or nitrate, on the carbon atom adjacent to the reacting functional group (β-substitution)[53] and at other locations. Experiments were therefore conducted with HN, βHN, and βCN probe compounds to investigate potential reactions with themselves, each other, a selection of compounds that included 6-hydroxy-5-decanone (βHK), 1,2-decanediol (βDiol), 5-hydroxy-2-pentanone (δHK), and 1-octanol (Alc), and SOA formed from α-pinene ozonolysis. Experiments were conducted in a single organic

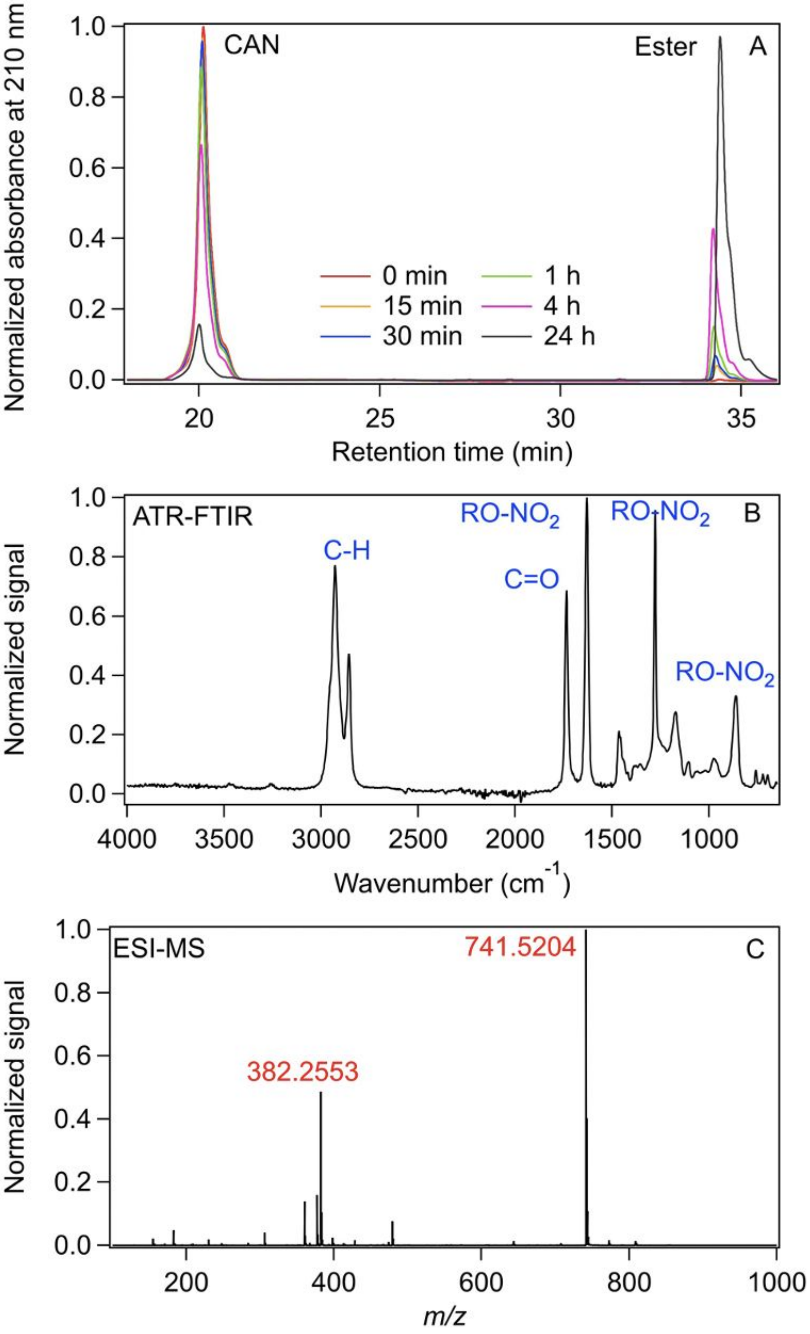

Figure 7. (A) Overlaid HPLC chromatograms measured during the 24 h reaction of CAN with 1-octanol to form an ester in a two-phase organic/aqueous mixture with the aqueous phase being a 3.0 M solution of sulfuric acid in water. Absorbance was measured at 210 nm and chromatograms were normalized to the CAN peak at 0 h. (B) ATR-FTIR spectrum measured for the collected ester HPLC fraction, where labelled peaks correspond to RO–NO$_2$ (1632.6, 1278.5, and 862.88 cm^{-1}), C=O (1735.1 cm^{-1}), and C–H (2927.8 cm^{-1}) stretches. (C) ESI mass spectrum measured for the collected ester HPLC fraction, where the peaks correspond to Na$^+$ adducts of the ester and a dimer formed in the ion source: [M + Na]$^+$ (382.2553) and [2M + Na]$^+$ (741.5204).

phase without sulfuric acid and in a phase-separated organic/aqueous mixture with sulfuric acid. The compounds used and potential reactions (not including those in SOA) are shown in Figure 8.

The results of these experiments are shown in Figures 9 and 10. In all experiments no reaction was observed over 24 h, regardless of whether reactants were present in a single organic phase without sulfuric acid or in a phase-separated organic/aqueous mixture with sulfuric acid. This was even the case for the reaction of CAN, which was observed to occur with 1-octanol in a phase-separated organic/aqueous mixture with sulfuric acid. For the most part, this is probably due to the lower concentration of hydroxyl groups in the SOA, which from or previous functional group analysis[40] are estimated to be 1.4 M compared to 6.4 M for 1-octanol. Overall, these results are surprising, in light of results from previous studies we and others have conducted on SOA formed in environmental chamber reactions.[13–19, 54] For example, in a study of SOA formed from reactions of 1-alkenes with OH radicals in the presence of NO_x we observed oligomers that appeared to be hemiacetals formed from reactions of dihydroxycarbonyls that contained β-hydroxycarbonyl moieties.[52] And in studies of SOA formed from the reactions of β-pinene[18] and Δ-3-carene[19] with NO_3 radicals we observed acetal and hemiacetal oligomers formed from reactions of hydroxynitrates and cyclic hemiacetals that contained β-hydroxynitrate and β- carbonylnitrate groups. The most obvious difference between those experiments and these is that in the environmental chamber experiments the oligomers formed in SOA particles, while in these experiments reactions were conducted in bulk solutions. One must therefore wonder if oligomer formation in SOA occurred at particle surfaces, which were not present in the bulk solution studies, and this increased reactivity. A number of recent studies have indicated that some types of reactions among organic compounds can be significantly accelerated in aerosol particles, an effect that depends on factors such as the rates of

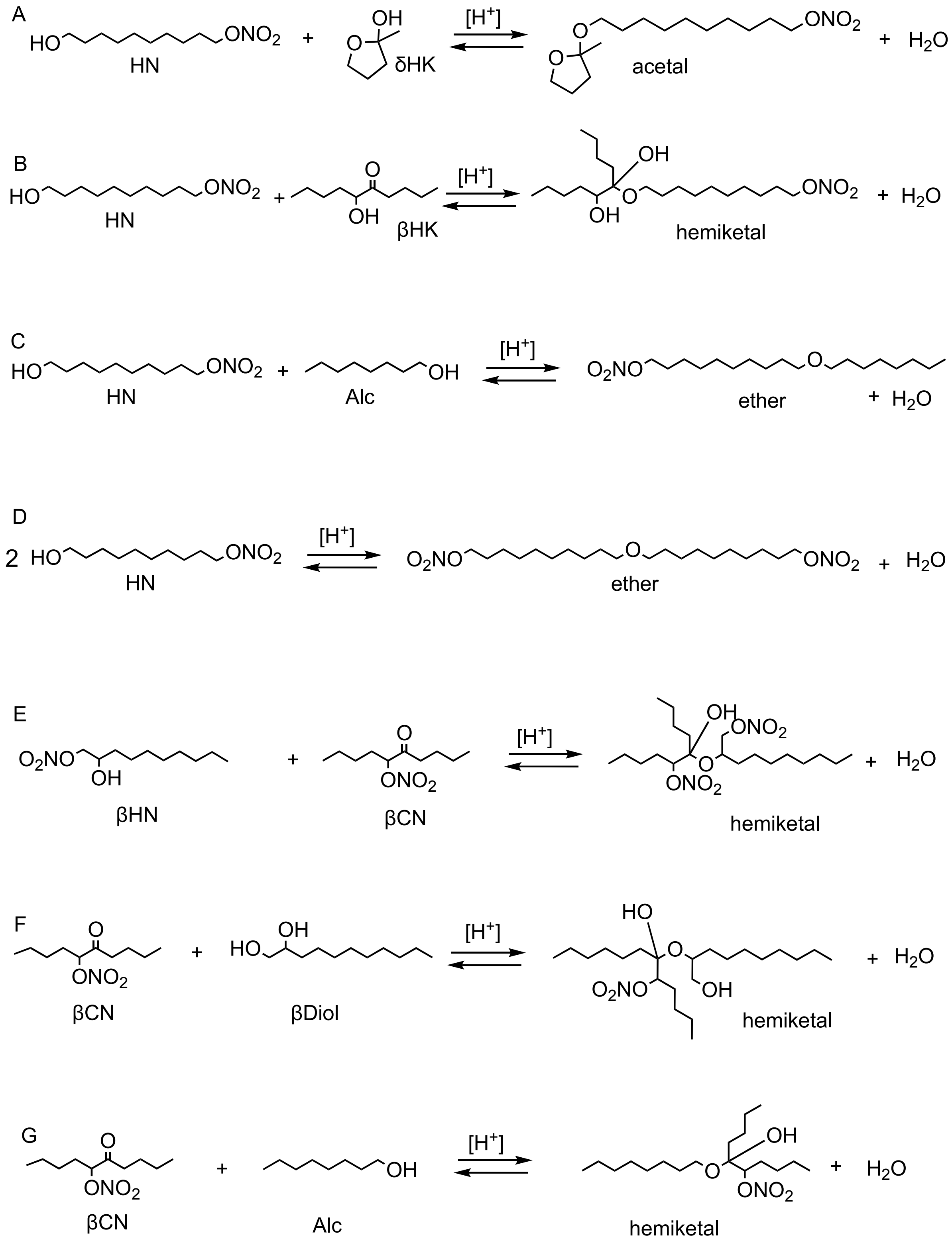

Figure 8. Potential acid catalyzed reactions of the following: HN with (A) 5-hydroxy-2-pentanone (δHK), (B) 6-hydroxy-5-decanone (βHK), (C) 1-octanol (Alc), and (D) another HN; (E) βHN with βCN; and βCN with (F) 1,2-butanediol (βDiol) and (G) 1-octanol (Alc).

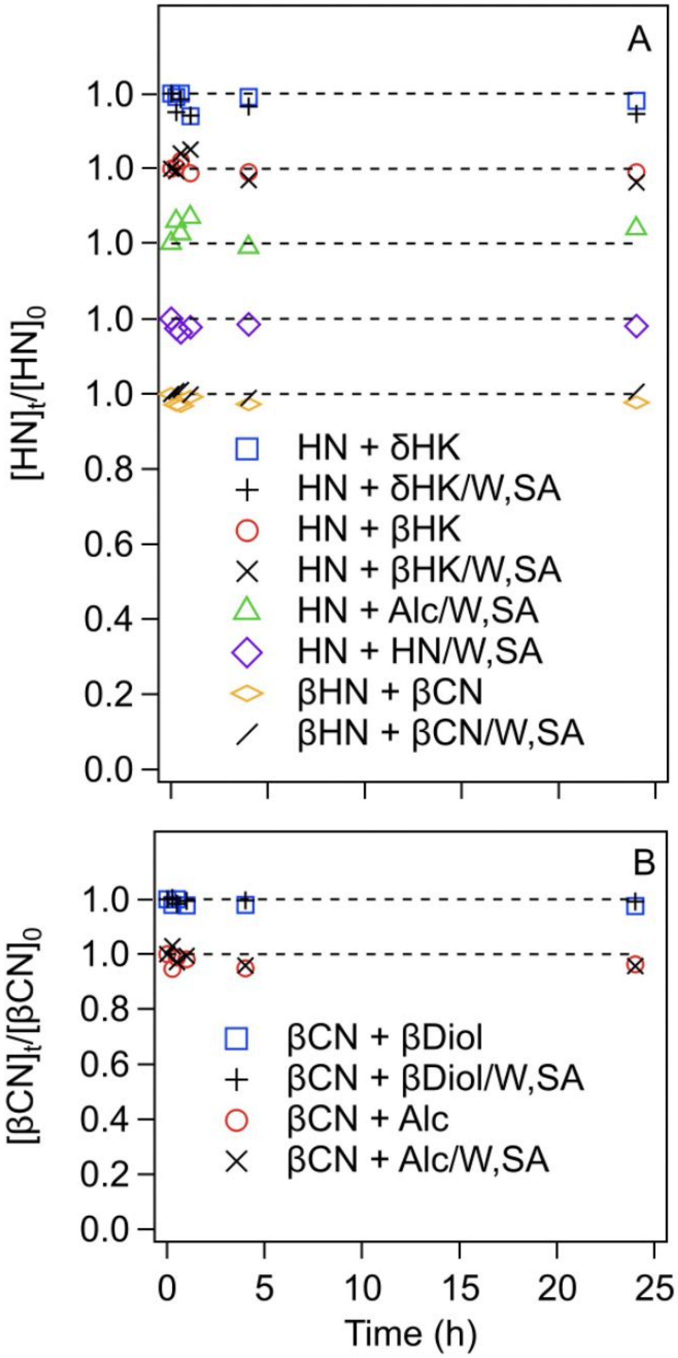

Figure 9. (A) Time profiles of the ratio $[HN]_t/[HN]_0$ for reactions of HN with 5-hydroxy-2-pentanone (δHK), 6-hydroxy-5-decanone (βHK), 1-octanol (Alc), itself (HN), and βCN; and time profiles of the ratio $[\beta HN]_t/[\beta HN]_0$ for reactions of βHN with βCN. (B) Time profiles of the ratio $[\beta CN]_t/[\beta CN]_0$ for reactions of βCN with 1,2-decanediol (βDiol) and 1-octanol (Alc). Reactions were conducted in either a single organic phase or a two-phase organic/aqueous mixture with the aqueous phase being a 3.0 M solution of sulfuric acid in water (W, SA). The dashed lines correspond to $[HN]_t/[HN]_0 = 1$, $[\beta HN]_t/[\beta HN]_0$, and $[\beta CN]_t/[\beta CN]_0 = 1$ and are offset to avoid crowding of data points. Results in panels A and B are for single experiments.

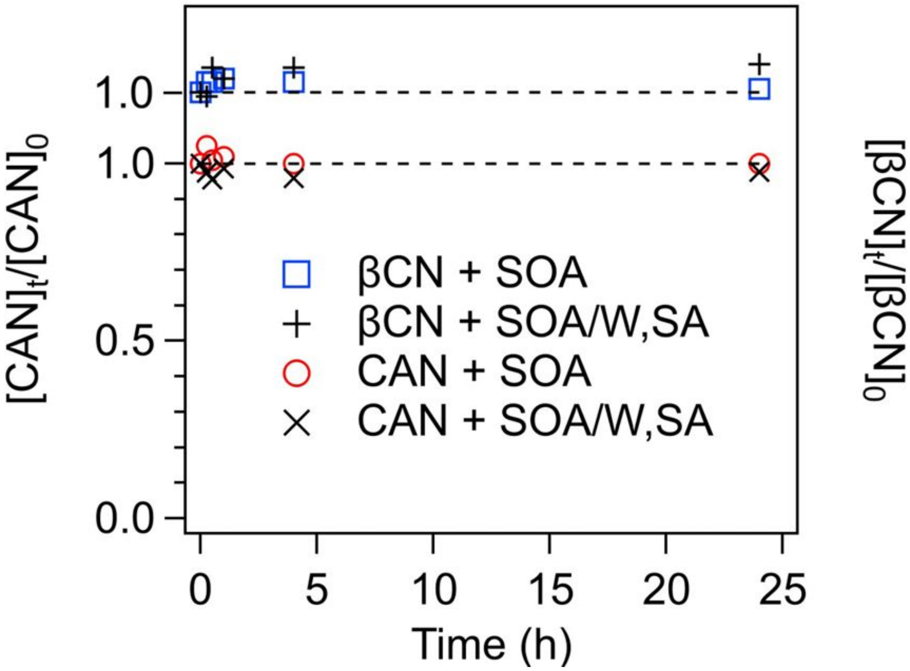

Figure 10. Time profiles of the ratio $[\beta CN]_t/[\beta CN]_0$ and $[CAN]_t/[CAN]_0$ for reactions of βCN and CAN with secondary organic aerosol (SOA) formed in the environmental chamber reaction of α-pinene with O_3 in either a single organic phase or a two-phase organic/aqueous mixture with the aqueous phase being a 3.0 M solution of sulfuric acid in water (W, SA). The dashed lines correspond to $[\beta CN]_t/[\beta CN]_0 = 1$ and $[CAN]_t/[CAN]_0 = 1$ and are offset to avoid crowding of data points. Results are for single experiments.

reaction in the surface region and bulk (which can be thought of as microcompartments), rates of transport in and out of the surface region, reactant concentrations, and particle size (which impacts the numbers of molecules in the surface region and bulk) .[55,56] It may also be that the more complex chemical composition of the SOA medium, compared to the simple solutions studied here, somehow enhances reaction rates.

We note that the reactions of simple alcohols with aldehydes to form hemiacetals, which have been shown to occur in solutions in the absence and presence of an acid catalyst,[57] have been difficult to investigate using our methods. For example, when the HN probe was mixed with nonanal or SOA under various conditions, the HN peak often decreased over time and a nearby peak grew in. When this product peak was collected, however, subsequent ESI-MS and

ATR-FTIR analysis indicated that the product decomposed before it could be detected. In other cases, no decay in the HN peak occurred and no product peak appeared. We attribute these results to reversible decomposition of the hemiacetal on a timescale that competes with HPLC analysis and fraction collection and analysis. This is consistent with results of a previous study in which we synthesized a C_{19} hemiacetal from the reaction of decanol and nonanal and added it to an environmental chamber as an aerosol by atomization.[58] By monitoring the particle mass spectrum in real time using a thermal desorption particle beam mass spectrometer, we then observed that the hemiacetal decomposed reversibly on a timescale of ~3 min.

4 Conclusions

Although it has been known for more than two decades that oligomers are a significant component of SOA, their structures, the mechanisms by which they are formed, and the rates of the responsible accretion reactions are still poorly understood. In the study described here, we sought to begin to address this problem by systematically investigating reactions of a large variety of compounds containing the functional groups most likely to be involved in atmospheric oligomer formation: hydroperoxide, hydroxyl, carboxyl, aldehyde, and ketone groups. Experiments were conducted in a single organic phase and in phase-separated organic/aqueous mixtures without and with a sulfuric acid catalyst in an attempt to simulate the range of aerosol acidity encountered in different regions of the globe.[31–33] The goal was to identify the most important SOA accretion reactions and their dependence on molecular structure, and to measure their kinetics and equilibrium constants.

The results of the study indicate that for the compounds investigated the most favorable accretion reaction is between hydroperoxides and aldehydes to form peroxyhemiacetals, which occurs rapidly even in the presence of competing water and the absence of an acid catalyst.

Consistent with results from our previous study of this reaction,[30] it is expected that peroxyhemiacetal equilibrium is achieved in SOA in about an hour, although it might be slower in glassy particles where diffusion is slow. It is likely that hemiacetal formation from the reaction of an alcohol and aldehyde occurs on a similar timescale, but apparently because of rapid reversible dissociation during our analyses we were unable to verify that this was the case. Reaction was also observed between a carboxylic acid and alcohol to form an ester in a single organic phase and in a phase-separated organic/aqueous mixture. But this required a sulfuric acid catalyst, and the presence of water significantly reduced the catalytic rate constant such that the time to reach equilibrium was on the order of a day. Furthermore, no reaction was observed when the carboxylic acid was mixed with SOA and allowed to react under similar conditions, apparently because of the lower concentration of reactive hydroxyl groups in the SOA. Much to our surprise, none of the other compounds investigated were observed to undergo accretion reactions, either in a single organic phase or in a phase-separated organic/aqueous mixture containing sulfuric acid. This was in spite of the fact that the compounds consisted not only of those with a single, potentially reactive functional group, but also multiple functional groups in locations that are known to enhance reactivity. These results are also in contrast with previous laboratory studies that convincingly identified esters, hemiacetals, acetals, and aldols in SOA,[13–19] even though in many cases water was present that would shift the reaction towards monomers and when acid was present its concentration was likely much lower than that used here. Although we did not investigate aldol formation, it is worth noting that Casale et al.[59] concluded from their studies of the kinetics of aldol condensation in reactions of a series of aliphatic aldehydes in highly concentrated solutions of sulfuric acid in water (65–85 weight %) that this reaction is too slow to be significant in the atmosphere.

The reasons for the discrepancies between results of experiments conducted in solutions and observations from laboratory studies of SOA are not obvious, but it may be that accretion reactions are accelerated at particle surfaces,[55,56] or that the SOA contains compounds with more reactive structures than those employed here. It is also important to note that most of the analyses of oligomers in SOA have employed ESI-MS, which only provides molecular formulas and is not quantitative, so the contributions of different oligomers to SOA mass are in most cases highly uncertain. Future work needs to investigate these questions in order to obtain data on accretion reaction mechanisms, kinetics, and equilibria for use in atmospheric models and for better understanding the fates of organic compounds in the atmosphere.

Conflicts of Interest

There are no conflicts of interest to declare.

Acknowledgements

This material is based on work supported by the Army Research Office under Grant W911NF-17-1-0607.

References

1. U. Pöschl, Atmospheric aerosols: Composition, transformation, climate and health effects, *Angew. Chem. Int. Ed.*, 2005, **44**, 7520–7540.
2. J. H. Seinfeld and S. N. Pandis, *Atmospheric chemistry and physics: From air pollution to climate change*, Wiley, 3rd edn., 2016.
3. J. Haywood and O. Boucher, Estimates of the direct and indirect radiative forcing due to tropospheric aerosols: A review, *Rev. Geophys.*, 2000, **38**, 513–543.
4. Q. Zhang, J. L. Jimenez, M. R. Canagaratna, J. D. Allan, H. Coe, I. Ulbrich, M. R. Alfarra,

A. Takami, A. M. Middlebrook, Y. L. Sun, K. Dzepina, E. Dunlea, K. Docherty, P. F. DeCarlo, D. Salcedo, T. Onasch, J. T. Jayne, T. Miyoshi, A. Shimono, S. Hatakeyama, N. Takegawa, Y. Kondo, J. Schneider, F. Drewnick, S. Borrmann, S. Weimer, K. Demerjian, P. Williams, K. Bower, R. Bahreini, L. Cottrell, R. J. Griffin, J. Rautiainen, J. Y. Sun, Y. M. Zhang, D. R. Worsnop, Ubiquity and dominance of oxygenated species in organic aerosols in anthropogenically-influenced Northern Hemisphere midlatitudes, *Geophys. Res. Lett.*, 2007, **34**, L13801.

5. J. de Gouw and J. L. Jimenez, Organic aerosols in the Earth's atmosphere., *Environ. Sci. Technol.*, 2009, **43**, 7614–7618.
6. R. Atkinson and J. Arey, Atmospheric degradation of volatile organic compounds, *Chem. Rev.*, 2003, **103**, 4605–4638.
7. A. B. Guenther, X. Jiang, C. L. Heald, T. Sakulyanontvittaya, T. Duhl, L. K. Emmons and X. Wang, The model of emissions of gases and aerosols from nature version 2.1 (MEGAN2.1): An extended and updated framework for modeling biogenic emissions, *Geosci. Model Dev.*, 2012, **5**, 1471–1492.
8. J. H. Kroll and J. H. Seinfeld, Chemistry of secondary organic aerosol: Formation and evolution of low-volatility organics in the atmosphere, *Atmos. Environ.*, 2008, 42, 3593–3624.
9. P. J. Ziemann and R. Atkinson, Kinetics, products, and mechanisms of secondary organic aerosol formation, *Chem. Sci. Rev.*, 2012, **41**, 6582–6605.
10. M. Hallquist, J. C. Wenger, U. Baltensperger, Y. Rudich, D. Simpson, M. Claeys, J. Dommen, N. M. Donahue, C. George, A. H. Goldstein, J. F. Hamilton, H. Herrmann, T. Hoffmann, Y. Iinuma, M. Jang, M. E. Jenkin, J. L. Jimenez, A. Kiendler-Scharr, W.

Maenhaut, G. McFiggans, T. F. Mentel, A. Monod, A. S. H. Prevot, J. H. Seinfeld, J. D. Surratt, R. Szmigielski and J. Wildt, The formation, properties and impact of secondary organic aerosol: current and emerging issues, *Atmos. Chem. Phys.*, 2009, **9**, 5155–5236.

11. H. J. Tobias and P. J. Ziemann, Thermal desorption mass spectrometric analysis of organic aerosol formed from reactions of 1-tetradecene and O_3 in the presence of alcohols and carboxylic acids, *Environ. Sci. Technol.*, 2000, **34**, 2105–2115.
12. H. J. Tobias, K. S. Docherty, D. E. Beving and P. J. Ziemann, Effect of relative humidity on the chemical composition of secondary organic aerosol formed from reactions of 1-tetradecene and O_3. *Environ. Sci. Technol.*, 2000, **34**, 2116–2125.
13. L. Müller, M.-C. Reinnig, J. Warnke, and Th. Hoffmann, Unambiguous identification of esters as oligomers in secondary organic aerosol formed from cyclohexene and cyclohexene/α-pinene ozonolysis, *Atmos. Chem. Phys.*, 2008, **8**, 1423–1433.
14. J. D. Surratt, S. M. Murphy, J. H. Kroll, N. L. Ng, L. Hildebrandt, A. Sorooshian, R. Szmigielski, R. Vermeylen, W. Maenhaut, M. Claeys, R. C. Flagan and J. H. Seinfeld, Chemical composition of secondary organic aerosol formed from the photooxidation of isoprene. *J. Phys. Chem. A*, 2006, **110**, 9665–9690.
15. T. B. Nguyen, P. J. Roach, J. Laskin, A. Laskin and S. A. Nizkorodov, Effect of humidity on the composition of isoprene photooxidation secondary organic aerosol, *Atmos. Chem. Phys.*, 2011, **11**, 6931–6944.
16. M. Kalberer, D. Paulsen, M. Sax, M. Steinbacher, J. Dommen, A. S. H. Prevot, R. Fisseha, E. Weingartner, V. Frankevich, R. Zenobi and U. Baltensperger, Identification of polymers as major components of atmospheric organic aerosols, *Science*, 2004, **303**, 1659–1662.

17. D. O. DeHaan, A. L. Corrigan, M. A. Tolbert, J. L. Jimenez, S. E. Wood and J. J. Turley, Secondary organic aerosol formation by self-reactions of methylglyoxal and glyoxal in evaporating droplets, *Environ. Sci. Technol*., 2009, **43**, 8184–8190.

18. M. S. Claflin and P. J. Ziemann, Identification and quantitation of aerosol products of the reaction of β-pinene with NO_3 radicals and implications for gas- and particle-phase reaction mechanisms, *J. Phys. Chem. A*, 2018, **122**, 3640–3652.

19. M. P. and P. J. Ziemann, Gas- and particle-phase products and their mechanisms of formation from the reaction of Δ-3-carene with NO_3 radicals, *J. Phys. Chem. A*, 2021, **125**, 10207–10222.

20. B. Aumont, S. Szopa, and S. Madronich, Modelling the evolution of organic carbon during its gas-phase tropospheric oxidation: development of an explicit model based on a self generating approach, 2005, *Atmos. Chem. Phys*. **5**, 2497–2517.

21. http://mcm.leeds.ac.uk/MCM/

22. Y. Im, M. Jang and R. L. Beardsley, Simulation of the aromatic SOA formation using the lumping model integrated with explicit kinetic mechanisms and aerosol phase reactions, *Atmos. Chem. Phys.*, 2014, **14**, 4013–4027.

23. T. P. Riedel, Y.-H. Lin, Z. Zhang, K. Chu, J. A. Thornton, W. Vizuete, A. Gold and J. D. Surratt, Constraining condensed-phase formation kinetics of secondary organic aerosol components from isoprene epoxydiols, *Atmos. Chem. Phys.*, 2016, **16**, 1245–1254.

24. M. Jenkin, Modelling the formation and composition of secondary organic aerosol from α- and β-pinene ozonolysis using MCM v3, *Atmos. Chem. Phys.*, 2004, **4**, 1741–1757.

25. Y. S. La, M. Camredon, P. J. Ziemann, R. Valorso, A. Matsunaga, V. Lannuque, J. Lee Taylor, A. Hodzic, S. Madronich and B. Aumont, Impact of chamber wall loss of gaseous

organic compounds on secondary organic aerosol formation: explicit modeling of SOA formation from alkane and alkene oxidation, *Atmos. Chem. Phys*., 2016, **16**, 1417–1431.

26. S. R. Utembe, L. A. Watson, D. E. Shallcross, M. E. Jenkin, A Common Representative Intermediates (CRI) mechanism for VOC degradation. Part 3: Development of a secondary organic aerosol module, *Atmos. Environ*. 2009, **43**, 1982–1990.

27. J. Lee-Taylor, S. Madronich, B. Aumont, M. Camredon, A. Hodzic, G. S. Tyndall, E. Apel and R. A. Zaveri, Explicit modeling of organic chemistry and secondary organic aerosol partitioning for Mexico City and its outflow plume, *Atmos. Chem. Phys*., 2011, **11**, 13219–13241.

28. Y. You, M. L. Smith, M. Song, S. T. Martin and A. K. Bertram, Liquid–liquid phase separation in atmospherically relevant particles consisting of organic species and inorganic salts, *Int. Rev. Phys. Chem*., 2014, **33**, 43–77.

29. A. K. Bertram, S. T. Martin, S. J. Hanna, M. L. Smith, A. Bodsworth, Q. Chen, M. Kuwata, A. Liu, Y. You and S. R. Zorn, Predicting the relative humidities of liquid-liquid phase separation, efflorescence, and deliquescence of mixed particles of ammonium sulfate, organic material, and water using the organic-to-sulfate mass ratio of the particle and the oxygen-to-carbon elemental ratio of the organic component, *Atmos. Chem. Phys*., 2011, **11**, 10995–11006.

30. J. G. Bakker-Arkema and P. J. Ziemann, Measurements of kinetics and equilibria for the condensed phase reactions of hydroperoxides with carbonyls to form peroxyhemiacetals, *ACS Earth Space Chem.*, 2020, **4**, 467–475.

31. H. O. T. Pye, A. Nenes, B. Alexander, A. P. Ault, M. C. Barth, S. L. Clegg, J. L. Collett Jr., K. M. Fahey, C. J. Hennigan, H. Herrmann, M. Kanakidou, J. T. Kelly, I-T. Ku, V. F.

McNeill, N. Riemer, T. Schaefer, G. Shi1, A. Tilgner, J. T. Walker, T. Wang, R. Weber, J. Xing, R. A. Zaveri, and A. Zuend, The acidity of atmospheric particles and clouds, 2020, *Atmos. Chem. Phys*. **20**, 4809–4888.

32. H. Guo, L. Xu, A. Bougiatioti, K. M. Cerully, S. L. Capps, J. R. Hite Jr., A. G. Carlton, S.-H. Lee, M. H. Bergin, N. L. Ng, A. Nenes and R. J. Weber, Fine-particle water and pH in the southeastern United States, 2015, *Atmos. Chem. Phys.* **15**, 5211–5228.

33. B. A. Nault, P. Campuzano-Jost, D. A. Day, D. S. Jo, J. C. Schroder, H. M. Allen, R. Bahreini, H. Bian, D. R. Blake, M. Chin, S. L. Clegg, P. R. Colarco, J. D. Crounse, M. J. Cubison, P. F. DeCarlo, J. E. Dibb, G. S. Diskin, A. Hodzic, W. Hu, J. M. Katich, M. J. Kim J. K. Kodros, A. Kupc, F. D. Lopez-Hilfiker, E. A. Marais, A. M. Middlebrook, J. A. Neuman, J. B. Nowak, B. B. Palm, F. Paulot, J. R. Pierce, G. P. Schill, E. Scheuer, J. A. Thornton, K. Tsigaridis, P. O. Wennberg, C. J. Williamson and J. L. Jimenez, Chemical transport models often underestimate inorganic aerosol acidity in remote regions of the atmosphere, 2021, Commun. Earth Environ. **2**, 93.

34. B. L. Deming and P. J. Ziemann, Measurements of the partitioning of nitric acid and sulfuric acid in aqueous/organic phase-separated systems, *Environ. Sci. Atmospheres*, 2021, **1**, 93–103.

35. R. Atkinson, C. N. Plum, W. P. L. Carter, A. M. Winer and J. N. Pitts, Rate constants for the gas-phase reactions of nitrate radicals with a series of organics in air at 298.+-. 1 K, *J. Phys. Chem.*, 1984, **88**, 1210–1215.

36. K. S. Docherty and P. J. Ziemann, Reaction of oleic acid particles with NO_3 radicals: Products, mechanism, and implications for radical-initiated organic aerosol oxidation, *J. Phys. Chem. A*, 2006, **110**, 3567–3577.

37. K. Taka´cs-Nova´k and A. Avdeel, Interlaboratory study of log P determination by shake-flask and potentiometric methods, *J. Pharm. Biomed. Anal.*, 1996, **14**, 1405–1413.

38. A. Paschke, P. L. Neitzel, W. Walther and G. Schüürmann, Octanol/water partition coefficient of selected herbicides: Determination using shake-flask method and reversed-phase high-performance liquid chromatography, *J. Chem. Eng. Data*, 2004, **49**, 1639–1642.

39. J. Williams, M. de Reus, R. Krejci, H. Fischer and J. Ström, Application of the variability-size relationship to atmospheric aerosol studies: Estimating aerosol lifetimes and ages, *Atmos. Chem. Phys.*, 2002, **2**, 133–145.

40. M. S. Claflin, J. E. Krechmer, W. Hu, J. L. Jimenez and P. J. Ziemann, Functional group composition of secondary organic aerosol formed from ozonolysis of α-pinene under high VOC and autoxidation conditions, *ACS Earth Space Chem.*, 2018, **2**, 1196–1210.

41. S. L. Clegg, P. Brimblecombe, and A. S. Wexler. A thermodynamic model of the system H^+ - NH_4^+ - Na^+ - SO_4^{2-} - NO_3^- - Cl^- - H_2O at 298.15 K. *J. Phys. Chem. A* 1998, **102**, 2155–2171.

42. A. S. Wexler and S. L. Clegg. Atmospheric aerosol models for systems including the ions H^+, NH_4^+, Na^+, SO_4^{2-}, NO_3^-, Cl^-, Br^-, and H_2O. *J. Geophys. Res.* 2002, **107**, D14.

43. R. M. Stephenson, Mutual solubility of water and aldehydes, *J. Chem. Eng. Data*, 1993, **38**, 630–633.

44. R. P. Bell and B. de B. Darwent, The kinetics of the hydration of acetaldehyde, *Trans. Farad. Soc.*, 1950, **46**, 34–41.

45. L. Deleebeeck, A. Snedden, D. Nagy, Z. Szilágyi Nagyne, M. Roziková, M. Viarová, A. Heering, F. Bastkowski, I. Leito, R. Quendera, V. Cabral and D. Stoica, Unified pH measurements of methanol, ethanol, and acetonitrile and their mixtures with water, *Sensors*, 2021, **21**, 3935.

46. B. E. Lang, Solubility of water in octan-1-ol (from 275 to 369) K, *J. Chem.Eng. Data*, 2012, **57**, 2221–2226.

47. R. A. Fairclough and C. N. Hinshelwood, The kinetics of the esterification of normal fatty acids, *J. Chem. Soc.*, 1939, 593–600.

48. A. A. Frost and R. G. Pearson, *Kinetics and mechanism*, John Wiley & Sons, Inc., 1953.

49. S. Z. Hassan and M. Vinjamur, Analysis of sensitivity of equilibrium constant to reaction conditions for esterification of fatty acids with alcohols, *Ind. Eng. Chem. Res.*, 2013, **52**, 1205–1215.

50. D. G. Lee, Y. Yongfei and W. David. Chandler, Measurement of equilibrium constants for the formation of esters from aliphatic carboxylic acids and alcohols, *Anal. Chem.*, 1994, **66**, 32–34.

51. H. Smith, Kinetics of the catalyzed esterification of normal aliphatic acids in methyl alcohol, *J. Am. Chem. Soc.*, 1939, **61**, 254–260.

52. Y. Liu, E. Lotero and J. G. Goodwin Jr., Effect of water on sulfuric acid catalyzed esterification, *J. Mol. Catal. A.: Chem*., 2006, **245**, 132–140.

53. R. Brucker, *Advanced organic chemistry*, Harcourt/Academic Press, 2002.

54. A. Matsunaga, K. S. Docherty, Y. B. Lim and P. J. Ziemann, Composition and yields of secondary organic aerosol formed from OH radical-initiated reactions of linear alkenes in the presence of NO_x: Modeling and measurements, *Atmos. Environ*., 2009, **43**, 1349-1357.

55. A. Fallah-Araghi, K. Meguellati, J.-C. Baret, A. E. Harrak,T. Mangeat, M. Karplus, S. Ladame, C. M. Marques and A. D. Griffiths, Enhanced chemical synthesis at soft interfaces: A universal reaction-adsorption mechanism in microcompartments, *Phys. Rev. Lett*., 2014, **112**, 028301.

56. K. R. Wilson, A. M. Prophet, G. Rovelli, M. D. Willis, R. J. Rapf and M. I. Jacobs, A kinetic description of how interfaces accelerate reactions in micro-compartments, *Chem. Sci.*, 2020, **11**, 8533–8545.

57. G. W. Meadows and B. de B. Darwent, The kinetics of the reactions of acetaldehyde with methanol. *Trans. Farad. Soc.*, 1952, **48**, 1015–1023.

58. M. S. Claflin and P. J. Ziemann, Thermal desorption behavior of hemiacetal, acetal, ether, and ester oligomers, *Aerosol Sci. Technol.*, 2019, **53**, 473–484.

59. M. T. Casale, A. R. Richman, M. J. Elrod, R. M. Garland, M. R. Beaver and M. A. Tolbert, Kinetics of acid-catalyzed aldol condensation reactions of aliphatic aldehydes, *Atmos. Environ.*, 2007, **41**, 6212–6224.